EIGHTEENTH EUROPEAN ROTORCRAFT FORUM

B-06

Paper N° 72

DEVELOPMENT AND VALIDATION OF A VORTEX LATTICE METHOD TO CALCULATE THE FLOW FIELD OF A HELICOPTER ROTOR INCLUDING FREE WAKE DEVELOPMENT

L. ZERLE, S.WAGNER
UNIVERSITÄT STUTTGART
GERMANY

September 15-18, 1992

AVIGNON, FRANCE

ASSOCIATION AERONAUTIQUE ET ASTRONAUTIQUE DE FRANCE

DEVELOPMENT AND VALIDATION OF A VORTEX LATTICE METHOD TO CALCULATE THE FLOWFIELD OF A HELICOPTER ROTOR INCLUDING FREE WAKE DEVELOPMENT

L. ZERLE and S. WAGNER
Institut für Aerodynamik und Gasdynamik
Universität Stuttgart
Pfaffenwaldring 21, D-7000 Stuttgart 80
Federal Republic of Germany

ABSTRACT

Calculated helicopter rotor inflow velocities in forward flight are presented and compared to laser doppler anemometer measurements. Basing on linear potential theory, the code works as a time-stepping simulation program, using vortex lattice method. Wake prolongation at blade trailing edge is performed during each timestep, shedding blade doublet strength into the wake. Additional wake self-induction is calculated and added to wake motion. Unsteady wake roll up, even at the inboard lattice parts, are observed. With the exception of the vortex core model, there is no empirical input to obtain the results. Improved blade vortex interaction (BVI) and rotor-fuselage interference predictions are the expected benefits of the free wake model. Comparisons demonstrate that the inflow velocity field is very well represented in tendency. Flow speed values in the outer radial rotor region also agree also well with measurement. Neglecting the missing fuselage in the calculation, results in differences at the inner rotor area.

1. INTRODUCTION

Progress in helicopter aerodynamics requires sufficient wake modelling. A wide span of problems stemming from the rotor wake is given by blade vortex interaction, aerodynamic noise production and vibratory loads. Compact and light helicopter construction requires knowledge about Rotor Fuselage Interference (RFI) effects, especially at canopy, rear rotor and fin area. Improved predictions in these cases are expected benefits by application of rotor free wake models. Increasing computer capabilities and arising CPU power under relative low costs allow application of aerodynamic rotor codes, working with fully free developed wake systems. A lot of research is published, using prescribed models for rotor downwash handling. They require empirical input data. Important for code development is an experimental database for comparisons and validation, to check the implied models. More than about 10 years, free wake technics are used in fixed wing applications, especially for delta wings [1]. Free wake methods are used in helicopter aerodynamics, too. Several research groups are working in this direction [2, 3]. Good historical review is given in the introductions of [4, 5].
Modern Laser Doppler Anemometry (LDA) flow measuring technics allow velocity measurements without placing any disturbing probe or hot wire equipment. Rotor inflow in forward flight was measured by NASA [6] using LDA. These results are used here for first comparisons with code calculations. The inhouse developed computer program for isolated rotor [7], was generally refined and expanded to forward flight within the Pilot Phase of BRITE EURAM research program [8]. Further measured data bases at different helicopter model sections were generated in this research phase, and will be used for comparisons in a later development step.

2. GENERAL CODE DESCRIPTION

Based on the theory of 3-dimensional linear potential flow, a vortex lattice method is used to determine time dependent flow field and wake geometry generation. The developed code is a timestep simulation program in FORTRAN 77 language. Flow conditions are calulated at every timestep, using the information of the former step to determine the new solution. Obtained timestep solu-

tions consit of two parts: 1. The local singularity strength at the blade panel, produced by fullfilling the boundary condition at the blade control points (i.e. no velocity perpendicular to the blade). 2. Displacement, prolongation and new positioning of the wake networks, which are locating the wake representing vorticies. During the timestep, quasi steady state potential flow conditions and a frozen geometry system are assumed, to calculate the new flow field and new wake geometry at the end of the timestep.

2.1 Coordinate Systems

Two coordinate systems are used. B–System is the blade fixed system, that represents the rotor blade in defined 0 – pitch angle position (Fig. 2.1). The other one, called System K is non rotating, rotorshaft axis and fuselage fixed, with location in the rotor center (Fig. 2.2). All calculations are performed in K system, fuselage and free stream are represented here also.

2.2 Blade Handling

For the first step thin blades were used, covered with a vortex doublet ring at every panel. At the blade control points all actual active velocities, i.e. free stream, wake induced, and rotor movement caused are added. After skalar multiplication of the velocity vectors with the unit vectors normal to the panel surface they build the right hand side of a system of linear equation.

$$\begin{bmatrix} a_{1,1} & a_{1,2} & \cdots & a_{1,N} \\ a_{2,1} & a_{2,2} & \cdots & a_{2,N} \\ a_{3,1} & a_{3,2} & \cdots & a_{3,N} \\ \vdots & \vdots & \ddots & \vdots \\ a_{N,1} & a_{N,2} & \cdots & a_{N,N} \end{bmatrix} \begin{bmatrix} \mu_1 \\ \mu_2 \\ \mu_3 \\ \vdots \\ \mu_N \end{bmatrix} = \begin{bmatrix} \mathcal{R}_1 \\ \mathcal{R}_2 \\ \mathcal{R}_3 \\ \vdots \\ \mathcal{R}_N \end{bmatrix}. \tag{1}$$

$$\mathcal{R}_k = -\vec{n}_k \cdot \Big(\underbrace{\vec{U}_\infty(\vec{r},t)}_{\textit{free stream}} - \underbrace{\vec{\Omega} \times \vec{r}_k}_{\textit{motion of rotorblade}} + \underbrace{\vec{\nabla}\phi_{VS}(\vec{r},t)}_{\textit{wake induced velocities}} \Big). \tag{2}$$

The blade panel doublet strength μ is determined by simultaneously solving the linear equation, using the blade–panel to blade–panel influence coefficient matrix a_{ki}, at the end of the timestep. Beginning each timestep, the complete rotor is generated by coordinate transformation and multiplication, regarding the actual pitch and flapping angles at the destinct blade positions.

2.3 Wake Handling

Wake discretisation is done by sheets of quadrilateral ring vorticies (wake doublets). Every two neighboured doublets build the vortex strength at the vortex filament between them, by balancing their doublet strength. Using this superposition, we obtain the well known 'horse shoe' vortex system of a lift producing wing with finite span. During every timestep a new wake row is produced at the blade trailing edge, where the KUTTA - condition is postulated. The new wake panels are shedded down from the blade with the same spanwise blade panel discretisation, and are loaded with the doublet strenght of the abuting blade trailing edge panels. Therefore, in case of a steady state moving wing, the vortex at blade's trailing edge is extinguished by balancing the doublet strength of blade and wake along the trailing edge. Unsteady wing movements, as usual in helicopter aerodynamics, cause alternating doublet strength on the blades. In this case the wake network is covered with a local varying doublet strength in quasi chord direction, and a vortex activity remains at the spanwise filaments. Doublet strength on each particular wake panel is kept constant during all timesteps.
For wake motion and distorsion during the timestep, displacement influence portion of free stream and every singularity (i.e. blade and wake vorticies) is calculated. Vortex induced displacement contributions are determined by application of a special transportation model, including the 3-dimensional BIOT - SAVART law. More detailed Information is given in chapter 2.6.1 and [9, 7].

2.4 Code Working Procedure

The code runs in the following way: After reading the input files and some precalculations the *timestep loop is entered*, with at first two steps for calculation of the startup. 0th. step: Rotor is in starting position, facing the freestream and the blade moving speed only.
1st. step: Rotor moves to new position and produces the first wake row in spanwise direction. The shedded doublet strength for the first wake *row is the blade doublet strength solution* obtained at step 0. Now the panel control points are affected by freestream, blade moving velocity

and the vorticies of the first panel row.
2nd. and further steps: Timestep loop works now in full configuration with additional displacement calculation at all free wake lattice nodal points. The wake length of each blade grows now step by step, influencing itself, too. Therefore, computing time increases timestep by timestep. At the end of each timestep loop specific output is written to a file for postprocessing. After the treatment of all scheduled timesteps final file output is done and the procedure ends. An additional illustration is given by the flowchart in Fig. 2.3

2.5 Timestep Length

Rotor speed and rotor moving angle step determine timestep length. Practicable angle steps depend on two details, wake shedding model and the desired result resolution in time and space. Concerning the applied wake prolongation model, increasing angle steps produce increasing misposition of wake vorticies nearby blade's trailing edge. The experience shows that 15 Degree rotor angle movement steps are acceptable. For special investigations a smaller angle step of 5 Degrees was used. A sensitivity test was done, to look how the results are affected by varying the timestep length. See chapter 3.2.4 .

2.6 Special View to Applied Models

Some model expansions are necessary, to avoid unrealistic flow conditions and to achive stability in the whole procedure.

2.6.1 Circular Transport of an Allocation Point by a Vortex Filament

Nature shows that a single vortex transports particles along a circle around its vortex core, and not along a line indicated by the tangential velocity direction. This prinziple [9] is used to model the transport mechanism in a vortex flow field (Fig. 2.4). The collocation point moves within the timestep along the circle from location Q to the target point P, depending on the circumferential speed given by the BIOT-SAVART law. Vector QP represents the displacement contribution of this vortex filament within the timestep, instead of a transversal dislocation to point P' away from the vortex core.

2.6.2 Vortex Core Model

Approaching to the vortex core, theory gives infinitely high induced circumferential speed, which is neither realistic nor observed in nature. Therefore a core model with exponential velocity damping is applied. It ensures steady velocity reduction down to zero, by approach to vortex core within the damping radius. This damping radius is the single empirical code input parameter. It is set to half of the minimum spanwise blade panel size.

3. RESULTS

3.1 Important Development Step Results

First forward fight calculations were performed with an untwisted testblade, used for blade panelisation testing and discretisation optimisation. The test run worked with constant rotor speed after impulsive start, with a moving angle of 15 degrees during each timestep, and an advance ratio of 0.20. Blade 1 of the 2-bladed rotor starts in rear positon, and the rotor completes the revolution after every 24 timesteps.

3.1.1 Wake Structure

Fig. 3.1 gives an impression about the wake geometry after the first rotor revolution. Typical outer (tip) vortex rolling up effects in the free wake are clear visible. The crossing of retreating blade 1 with the wake of blade 2 is remarkable, too. Blade 1 hits the tip vorticies nearly parallel at timestep 19. Wake plots in fig. 3.2 represent the actual wake structure after 3 rotor revolutions. Wake lattice distorts heavily, but a kind of systematical wake wrapping is obsered. The wake activity on the starboard side (positive y-area) is not symmetric to the other one. This demonstrates the necessity to include cyclic pitch capability to the rotor free wake code.

3.1.2 Blade Doublet Strength Oscillations

Calculated doublet strength of blade 1 is shown in isoline plot (Fig. 3.3a). After the start at t=0 up to time step 28 the doublet strength is dominated by a startup process in the flowfield. The following rotation cycles show very similar patterns in this diagram. Doublet strength versus time step at relative radial position (0.8 R) is detailed in figure 3.3b. This line diagram can be

subdivided to 3 typical areas:

1) Startup process until timestep 28 (i.e. first revolution) 2) Line peak, if the blade is in advancing position (timestep 30, 54 and 78) 3) Wake influenced doublet strength oscillations, if the blade passes by or crosses the wake in the rear rotor disk section.

Such fast 1-period oscillations as calculated during the time steps 42-50 and 66-74 are typical indications for noise generation ation, induced by wake – blade interference. That is one of the main results of this free wake rotor code.

3.2 Code Run and Results Comparison Using the 2MRTS Rotor

3.2.1 Measured Inflow Data Base

Published LDA data from NASA–Langley consist of rotor inflow data, measured one chord length above the tip path plane (TPP). The windtunnel model is a full rotor fuselage configuration, with 0.86 m rotor radius. It was tested at three different advance ratios (0.15, 0.23, 0.30). According to [6] the rotor was trimmed to a condition without blade flapping. Published velocities are already preprocessed by subtraction of the free stream component, and by relating to the blade tip speed. Two velocity components are given:
1. LAMDA – value represents the velocity component in perpendicular direction to the TPP (positive is upwind in postive z–direction).
2. MUE - value is a tip speed related velocity component, directed simultaneous parallel to TPP and x–z plane of the K–coordinate system (positive in rear direction).

The given time averaged measurement data were used for code result comparison. Also given instantaneous data will be used for further investigations.

3.2.2 Blade Discretisation

The twisted 2MRTS blade is modeled flat with 14 panels spanwise and 1 panel chordwise. The aerodynamic panels are shifted 0.25 chordlength downsteam, to position the blade bounded spanwise vortex on the 0.25 chord position and the blade control point to the 0.75 chord position. The panels are non equispaced, to obtain a good spanwise vortex strength resolution. Fig. 2.1

3.2.3 Code Run with 2-Bladed Rotor

A 2MRTS rotor with two baldes was calculated at an advance ratio of 0.15 for one rotor revolution, to see how the wake develops during startup situation. Two blades were used only, keeping a good overview with respect to the wake lattice (Fig. 3.4). In forward flight, tip vortex rollup at retreating blade side is similar strong at advancing blade side. That's a cyclic pitch effect. Additional to the tip vortex rollup, we also see rolling up activity at the inboard wake structures.

3.2.4 4-Bladed Rotor Application

Next investigations were performed with 4 blades, running 4 rotor revolutions. Using constant timesteps with 15 degrees stepwise rotor movment, 96 timesteps must be calculated. A fully free developed wake is shown in figure 3.5a . All four wakes wrap heavily into each other. About one and a half revolutions behind the rotor position the helical lattice structure is dissolved. A kind of global tip vortex rollup remains at the longitudinal border lines of the total wake system. The extracted wake part of a single blade (Fig. 3.5b) underlines the disintegration of the vortex lattice. It is important that the simulated wake system shows stable behaviour and no wake exploding occurs.
Blade doublet strength development versus time is given in four diagrams, one for each blade (Fig. 3.6). After the startup process the isoline pattern of all four blades are equal, with respect to phase displacement. That is a further demonstration that the simulation code works stable.

Timestep length variation effects were investigated by a special test run. Two revolutions after start, the timestep length was derated from 15 degrees to 5 degrees, to calculate the next quarter rotor turn. After that, the timestep length was switched back to 15 degrees. Blade 1 doublet strength devolpment of this special run was now compared to a normal run, using 15 degree timestep only. Isoline diagrams of both test cases (Fig. 3.7) show, that in the timespace after the slow down procedure the same doublet strength pattern is produced. Corresponding timestep numbers for the same rotor position are 66 with, and 54 without timestep length variation.
Result: Shorter timesteps increase the resoltion,

but don't cause changes in the wake system. Different solutions on the rotor blades during the follow–on timesteps were not observed.

First investigations of aerodynamic coupling effects were done, by including a simple body configuration to the isolated rotor code. The actual chosen body for this test is a half-infinite one. It is built by one point source under freestream only, simulating a rotation symmetric body (Fig. 3.8) Position and dimensions are similar to the real used wind tunnel model.

3.3 Rotor Inflow Data Comparisons

Calculation results of mean LAMDA and MUE are presented in disk diagrams with isolines to give an overview (Fig. 3.9–3.10), and in x–y like diagrams at distinct radial and circumferential positions (Fig. 3.11–3.13) to show the results in detail. Values in the plots represent NASA–Langley measurements (NL Meas.), free wake isolated rotor (FW Calc.) calculations and free wake results with simple body simulation by a single point source (FW +Body). Investigations were performed for three different advance ratios: 0.15, 0.23, 0.30 . A complete set of all result diagrams is given in [10].

3.3.1 Lamda Results

Isoline patterns look very similar to their measured counterparts. Unsymmetric downwash in the rear disk area is also represented as the tip vortex induced upwash in the disk front section. This observed similarity indicates that the wake vortex system is calculated well. Local differences between measured and calculated data are visible in line diagrams (Fig. 3.11–3.13). In the outer radial disk area the isolated rotor calculations agree with the NASA full configuration (i.e. rotor and fuselage) measurements. At the inner areas the calculated Lamda values are lower, but it is important that they follow the measured result line in the same tendency. If we take into account, that there is no panelised displacement body used in the calculations, the theoretical results are too low, which is correct.
Local improvements were achieved by application of the body simulating 3D-point source. In the disk front area, especially at 180 degree and $r/R < 0.5$ (Fig. 3.11c, 3.12c) the point source activity 'lifts' the lamda very near to the measured value. This result is qualitative only, and was a first study of fuselage to rotor influece.

3.3.2 MUE Results

Line diagrams of mue value (Fig. 3.13) show in radial direction the same tendency between measurement and calculation. Compared to lamda results the tendential agreement is weaker, and the relative difference is higher. A probable explanation is the following: Mue values are very sensitive to the vortex z–position in the K–coordinate system. Wake vorticies with high activity (i.e. blade tip vortex) are almost parallel to the rotor disk. Small differences in the z– position affect the Mue value strongly. Additional simple body simulation don't ensure result improvement. Tendential improvements are sometimes observed in the diagrams.

4. Conclusions

Free wake method application to rotor aerodynamics improve basic knowledge of rotor wake behaviour and its influence to other rotorcraft components. The achieved conformity between rotor inflow calculations and experiment indicate, that even details of the wake induced flowfield are represented well. First coupling attempts with a simple fuselage simulation show local improvement. Code expansion to a paneled fuselage with full rotor–wake coupling is necessary, to obtain important wake effects at fuselage surface.

References

[1] D. Levin and J. Katz. *Vortex-Lattice Method for the Calculation of the Nonsteady Separated Flow over Delta Wings. Journal of Aircraft*, 18(12):1032–1037, December 1981.

[2] G.L. Crouse, Jr., J.G. Leishman, and Napei Bi. *Theoretical and Experimental Study of Unsteady Rotor/Body Aerodynamic Interactions. Journal of the American Helicopter Society*, 37(1):55–65, January 1992.

[3] D.R. Clark and B. Maskew. *A Re-Examination of the Aerodynamics of Hovering Rotors Including the Presence of the Fuselage.* In *International Technical Specialists' Meeting on Rotorcraft Basic Research*, Atlanta, GA, 30332 USA, March 1991.

[4] A. Baron, M. Boffadossi, and S. De Ponte. *Numerical Simulation of Vortex Flows Past Impulsively Started Wings.* In *AGARD Fluid Dy-*

namics Panel Symposium, Scheveningen, Netherlands, October 1990. Paper 33.

[5] D.R. Clark and B. Maskew. *Calculation of Unsteady Rotor Blade Loads and Blade/Fuselage Interference.* In *Second International Conference on Rotorcraft Basic Research*, University of Maryland, College Park, Maryland USA, February 1988.

[6] J.W. Elliott, S.L. Althoff, and R.H. Sailey. *Inflow Measurement Made with a Laser Velocimeter on a Helicopter Model in Forward Flight.* Technical Memorandum TM 100541–100543, NASA Langley Research Center, Hampton, Virgina 23665–5225, 1988.

[7] A. Röttgermann, R. Behr, Ch. Schöttl, and S. Wagner. *Calculation of Blade-Vortex Interaction of Rotary Wings in Incompressible Flow by an Unsteady Vortex-Lattice Method Including Free Wake Analysis.* In Hackbusch W., editor, *Notes on Numerical Fluid Mechanics*, pages 153–166, Braunschweig, 1991. Vieweg Verlag.

[8] L. Zerle and S. Wagner. *Progress Reports in BRITE EURAM Aero 0011 C(A) 'SCIA' Project 1990–1992.* Technical report, Institut für Luftfahrttechnik und Leichtbau, Universität der Bundeswehr München, 8014 Neubiberg, Germany, 1991.

[9] R. Behr and S. Wagner. *A Vortex-Lattice Method for the Calculation of Vortex Sheet Roll-Up and Wing-Vortex Interaction.* In E.H. Hirschel, editor, *Finite Approximations in Fluid Mechanics II*, volume 25, pages 1–13. Friedr. Vieweg & Sohn, Braunschweig und Wiesbaden, 1989.

[10] L. Zerle and S. Wagner. *Final Technical Report BRITE EURAM Aero 0011 C(A) 'SCIA' Project 1990–1992.* Technical report, Institut für Luftfahrttechnik und Leichtbau, Universität der Bundeswehr München, 8014 Neubiberg, Germany, 1992.

[11] A. Lesching and S. Wagner. *Theoretical Model to Calculate Aerodynamic Interference Effects between Rotor and Wing of Tiltrotors.* In *Proceedings of the 16. European Rotorcraft Forum*, Glasgow,UK, September 1990. Paper No. 11.2.

[12] O.A. Kandil. *Steady and Unsteady Incompressible Free-Wake Analysis.* In L. Morino, editor, *Computational Methods in Potential Aerodynamics*, pages 631–677. Springer Verlag, Berlin, 1985.

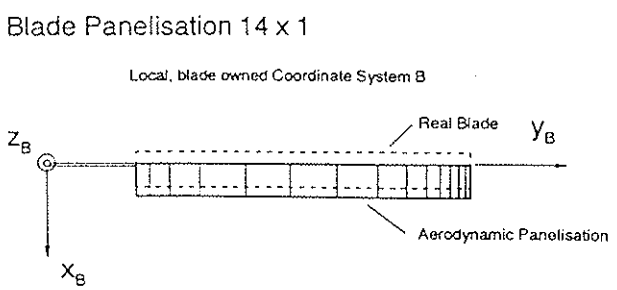

Fig. 2.1

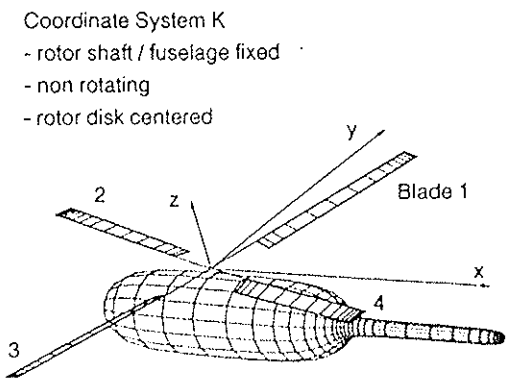

Fig. 2.2

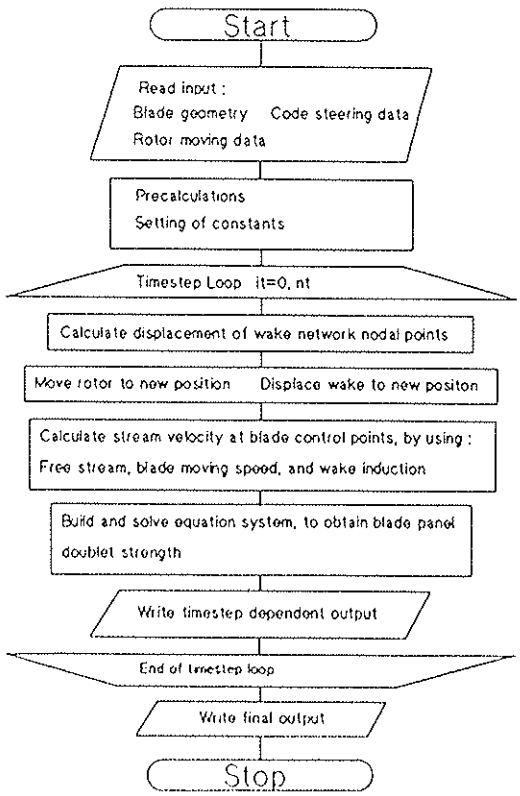

Fig. 2.3

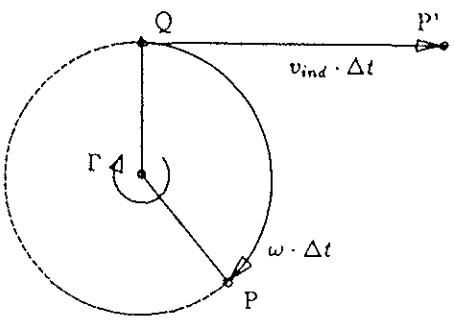

Fig. 2.4

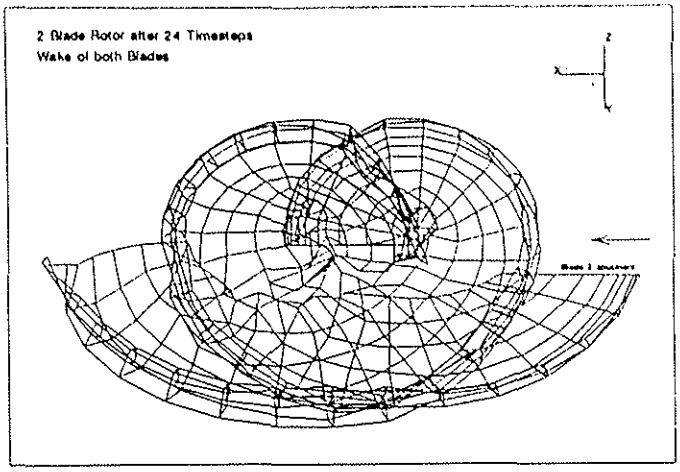

Fig. 3.1

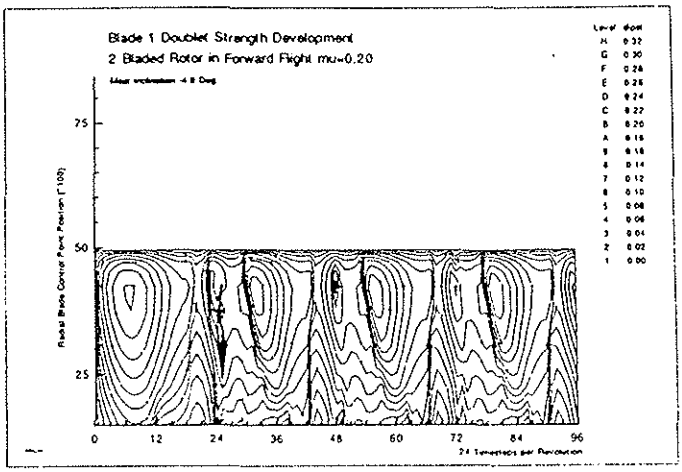

Fig. 3.3a

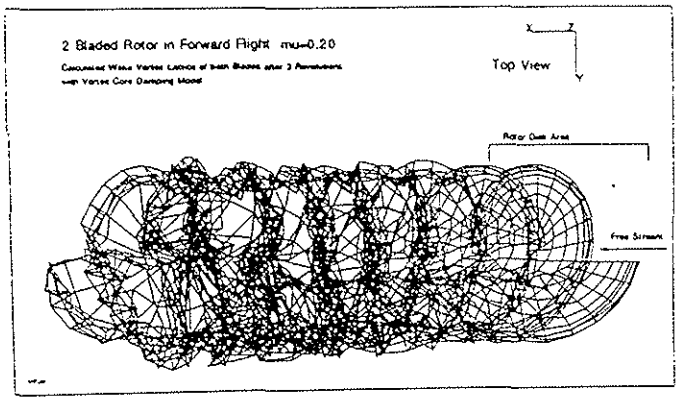

Fig. 3.2

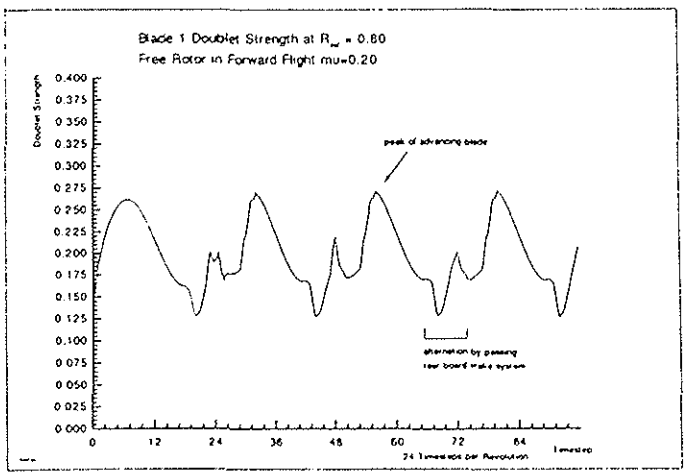

Fig. 3.3b

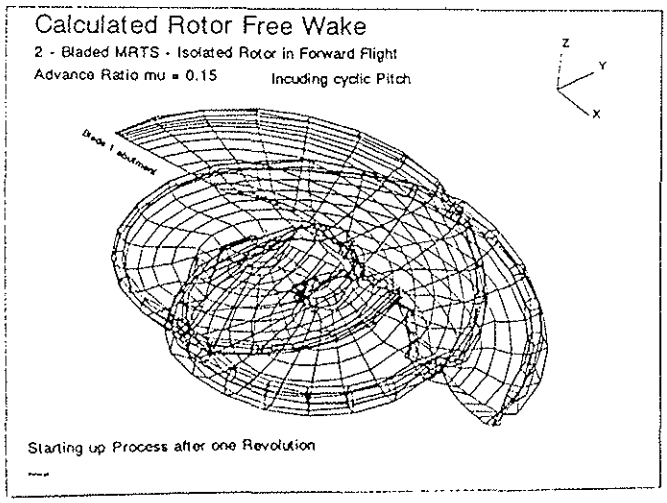

Fig. 3.4

Wake of 4-Bladed Rotor after 4 Revolutions mu = 0.23

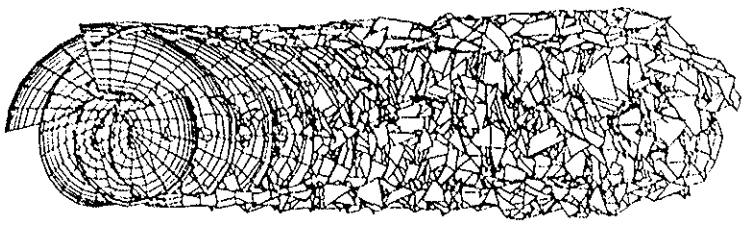

Fig. 3.5a

Wake of Blade No.3 only

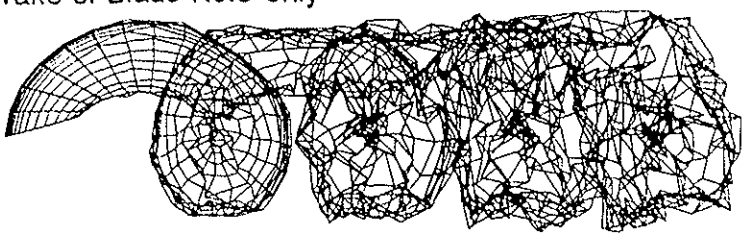

Fig. 3.5b

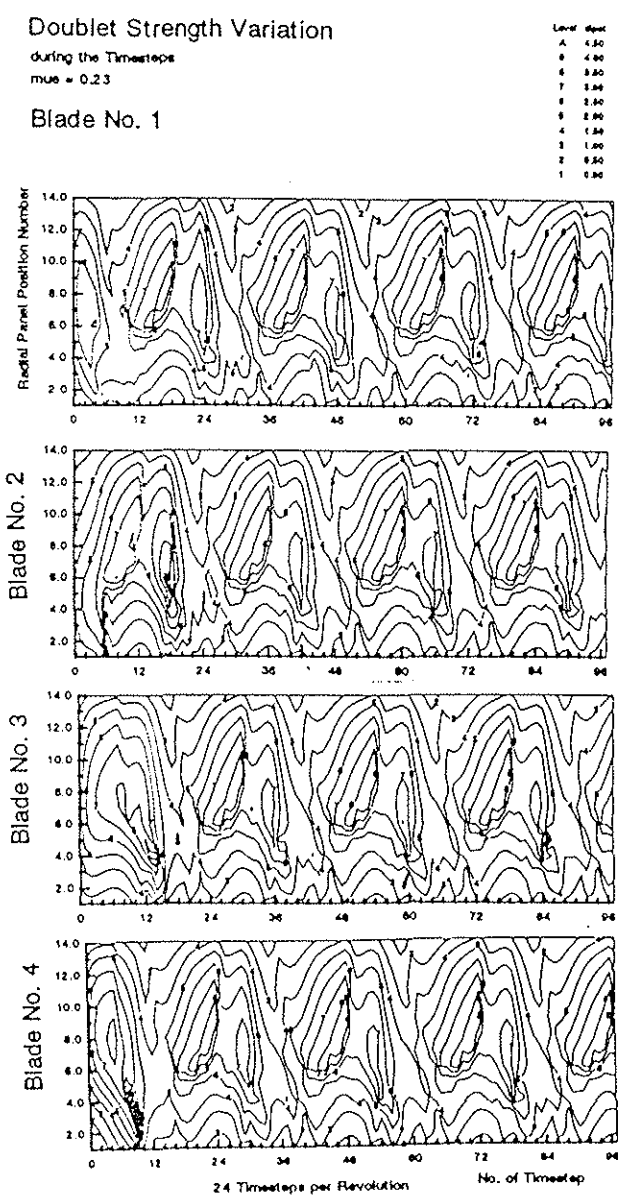

Fig. 3.6

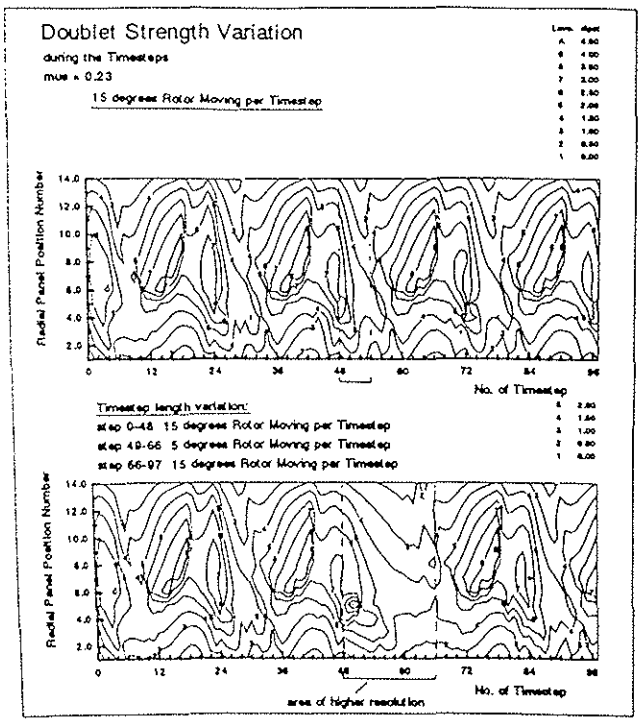

Fig. 3.7

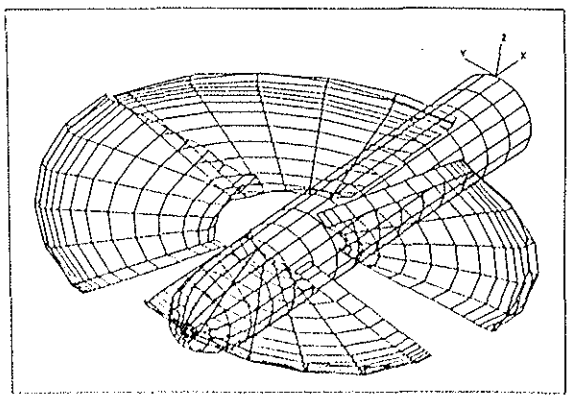

Fig. 3.8

Mean Rotor Inflow Data

Free Wake Calculaion

Lamda Isolines v_{ind} / v_{tip}

Advance Ratio mu = 0.23

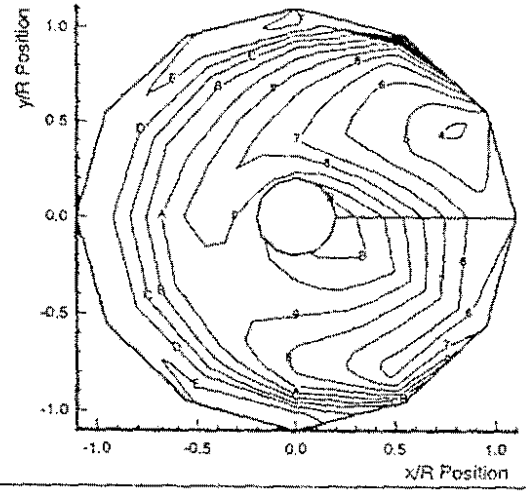

Level	LAMBD
H	0.0250
G	0.0200
F	0.0150
E	0.0100
D	0.0050
C	-0.0000
B	-0.0050
A	-0.0100
9	-0.0150
8	-0.0200
7	-0.0250
6	-0.0300
5	-0.0350
4	-0.0400
3	-0.0450
2	-0.0500
1	-0.0550

3.10a

Mean Rotor Inflow Data

NASA - Langley Measurement

Lamda Isolines v_{ind} / v_{tip}

Advance Ratio mu = 0.23

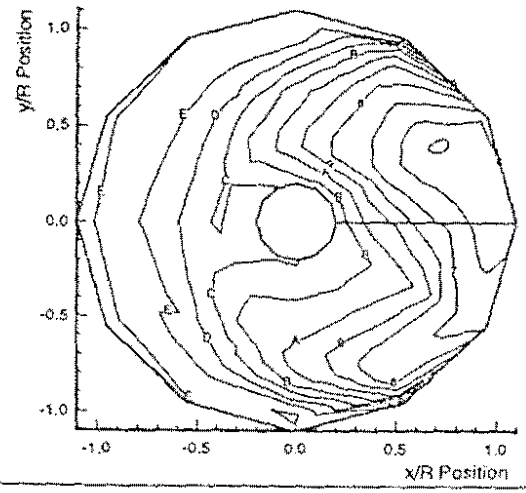

Level	LAMBD
H	0.0250
G	0.0200
F	0.0150
E	0.0100
D	0.0050
C	-0.0000
B	-0.0050
A	-0.0100
9	-0.0150
8	-0.0200
7	-0.0250
6	-0.0300
5	-0.0350
4	-0.0400
3	-0.0450
2	-0.0500
1	-0.0550

3.10b

Mean Rotor Inflow Data

Free Wake Calculaion

Lamda Isolines v_{ind} / v_{tip}

Advance Ratio mu = 0.15

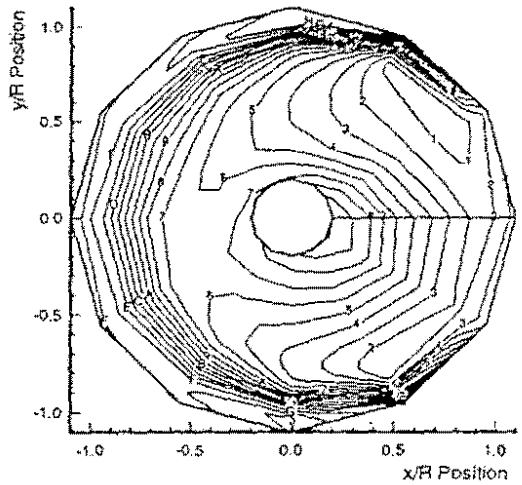

Level	LAMBD
H	0.0250
G	0.0200
F	0.0150
E	0.0100
D	0.0050
C	-0.0000
B	-0.0050
A	-0.0100
9	-0.0150
8	-0.0200
7	-0.0250
6	-0.0300
5	-0.0350
4	-0.0400
3	-0.0450
2	-0.0500
1	-0.0550

3.9a

Mean Rotor Inflow Data

NASA - Langley Measurement

Lamda Isolines v_{ind} / v_{tip}

Advance Ratio mu = 0.15

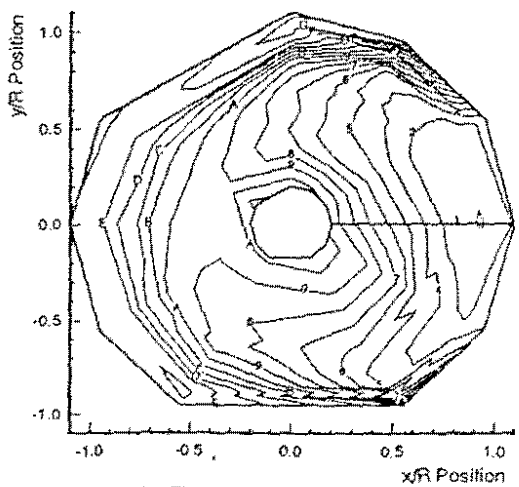

Level	LAMBD
H	0.0250
G	0.0200
F	0.0150
E	0.0100
D	0.0050
C	-0.0000
B	-0.0050
A	-0.0100
9	-0.0150
8	-0.0200
7	-0.0250
6	-0.0300
5	-0.0350
4	-0.0400
3	-0.0450
2	-0.0500
1	-0.0550

3.9b

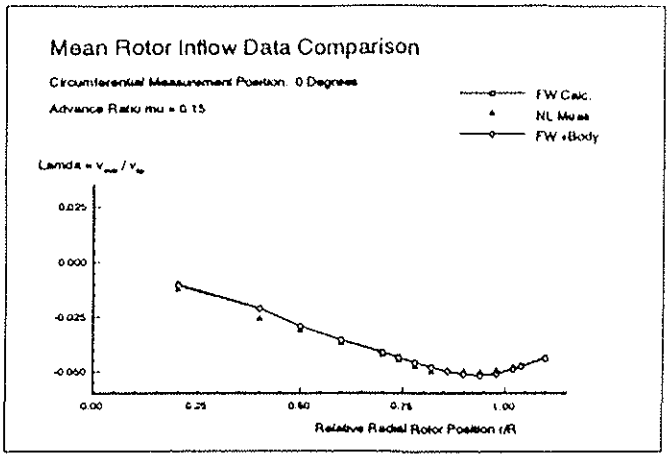

a

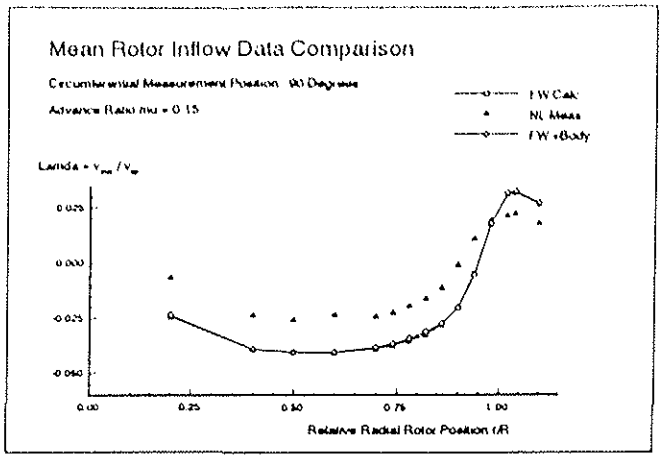

b

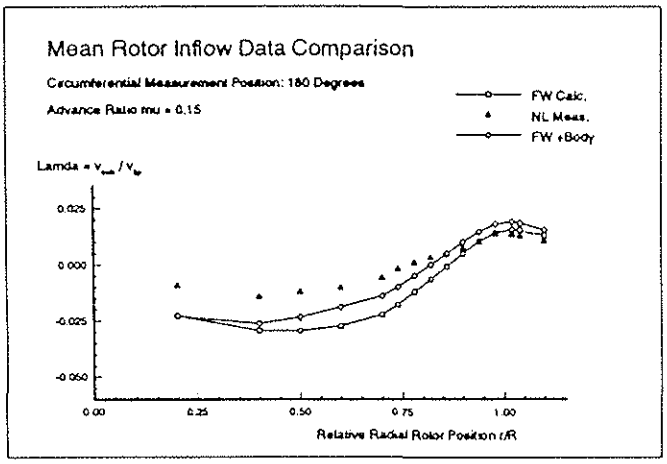

c

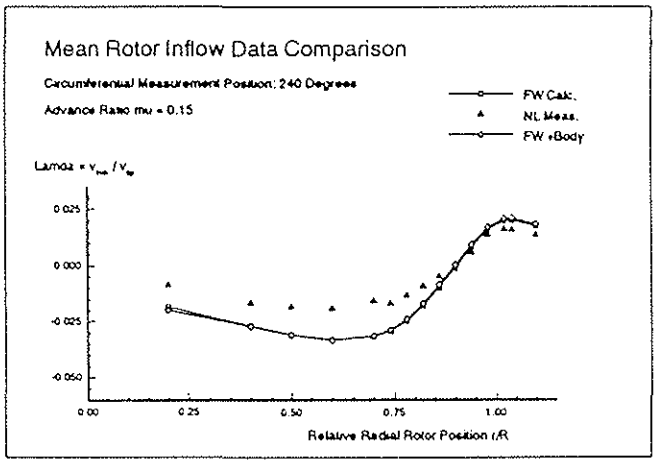

d

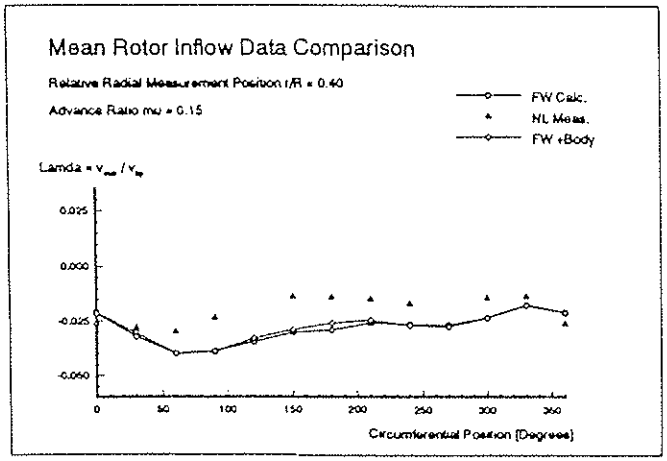

e

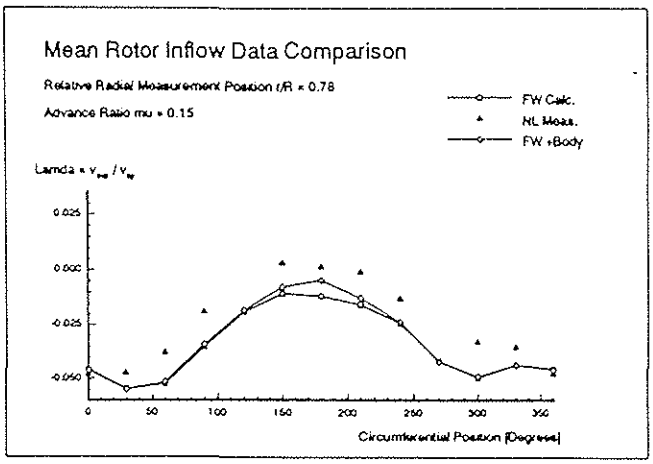

f

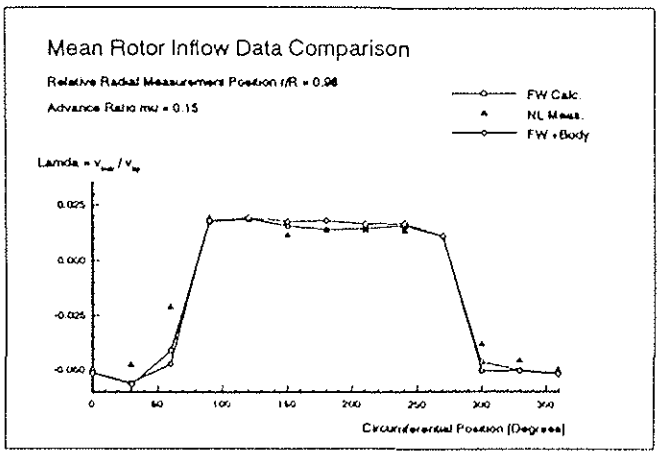

g

Figure 3.11

LAMDA - Inflow Data

Vertical to Tip Path Plane)

Advance Ratio 0.15

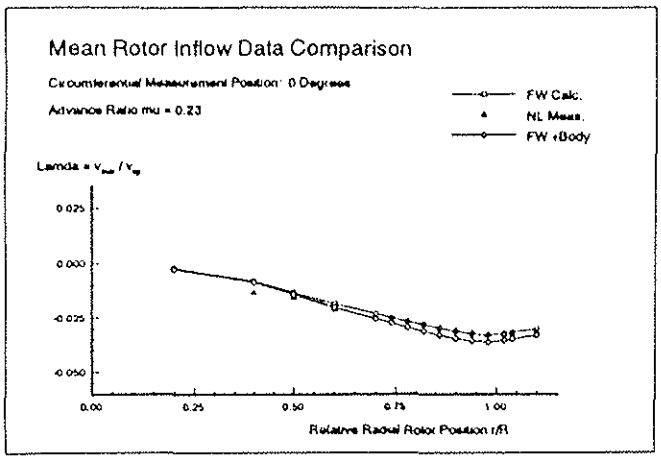

a

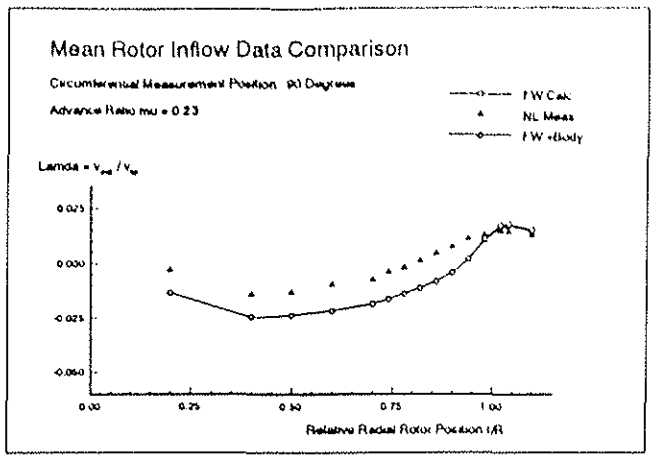

b

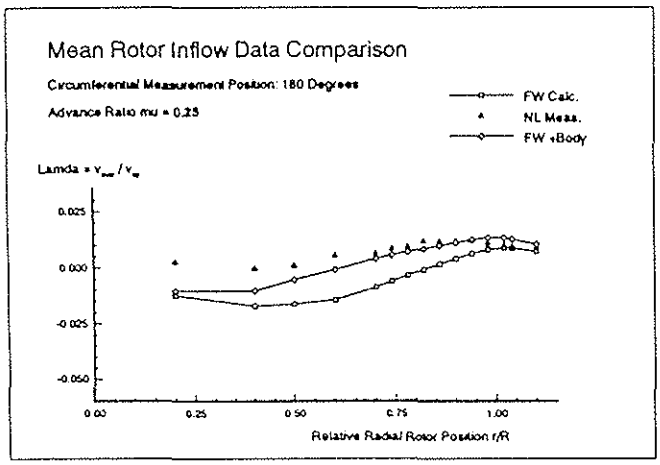

c

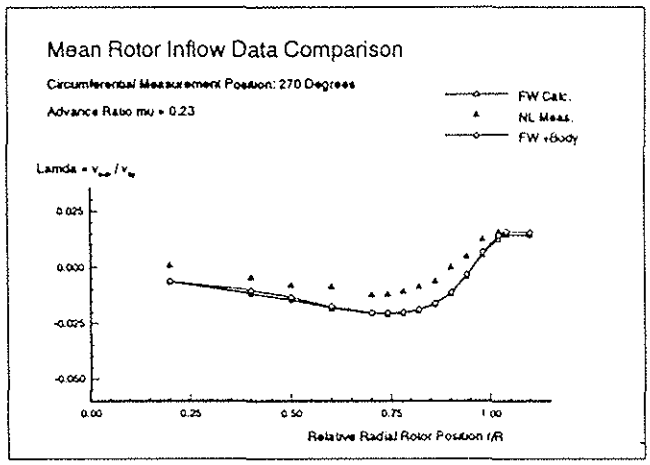

d

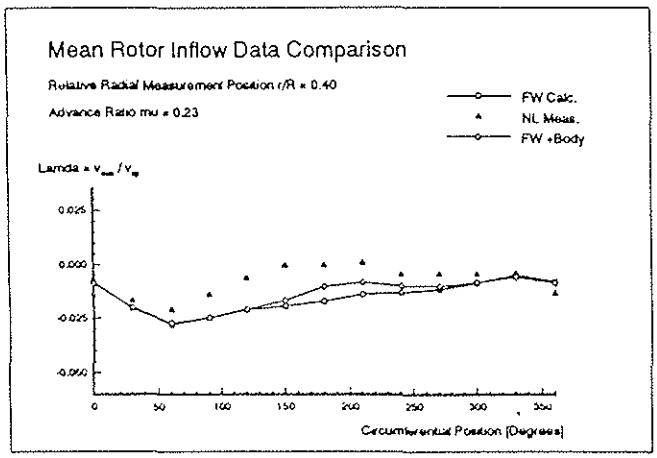

e

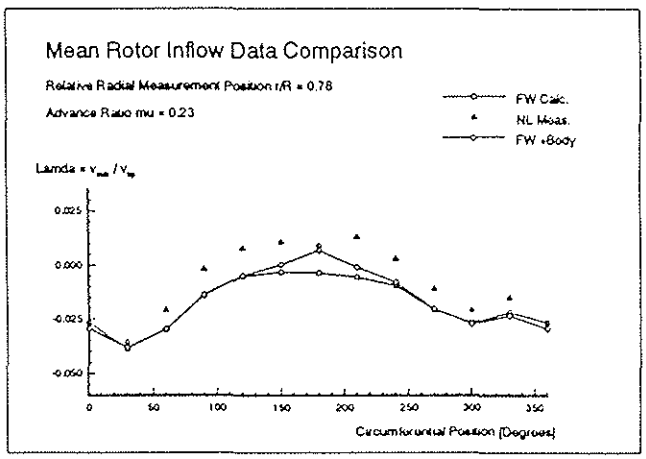

f

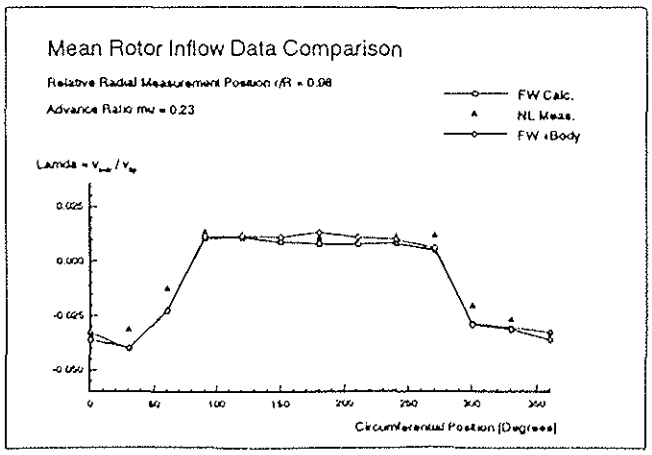

g

Figure 3.12

LAMDA - Inflow Data

(Vertical to Tip Path Plane)

Advance Ratio 0.23

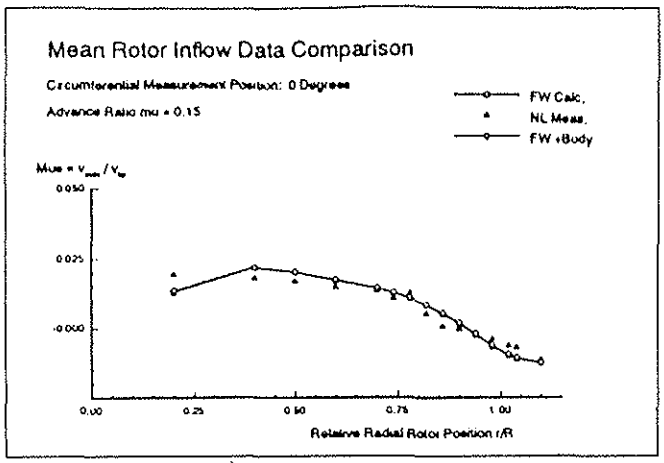

a

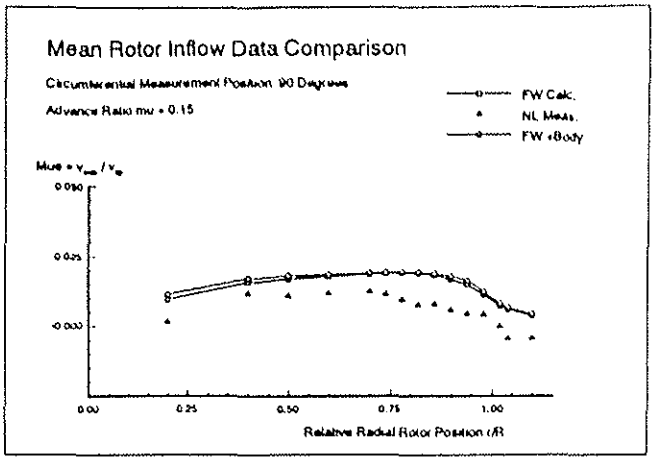

b

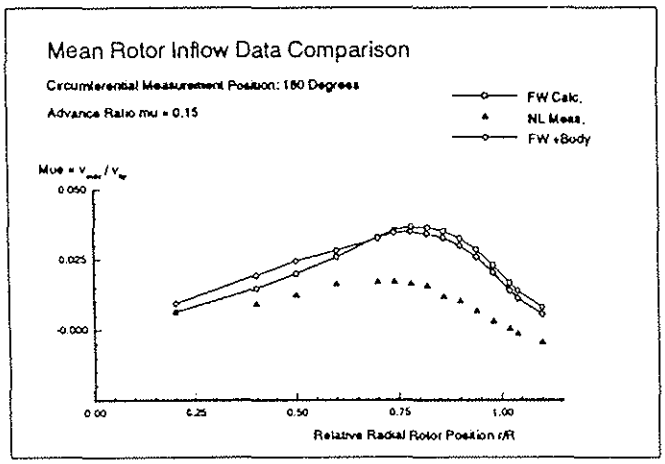

c

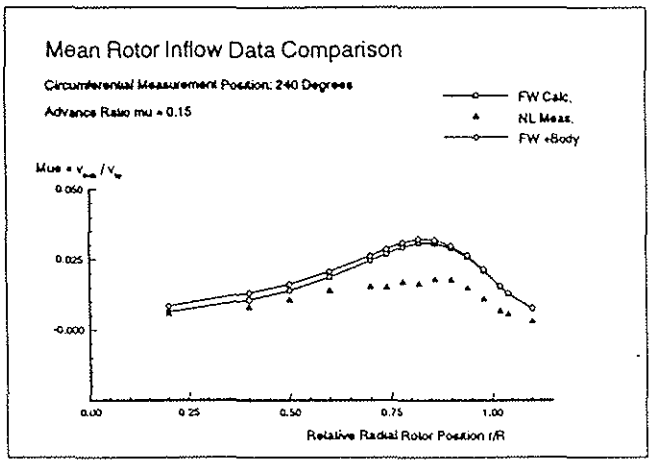

d

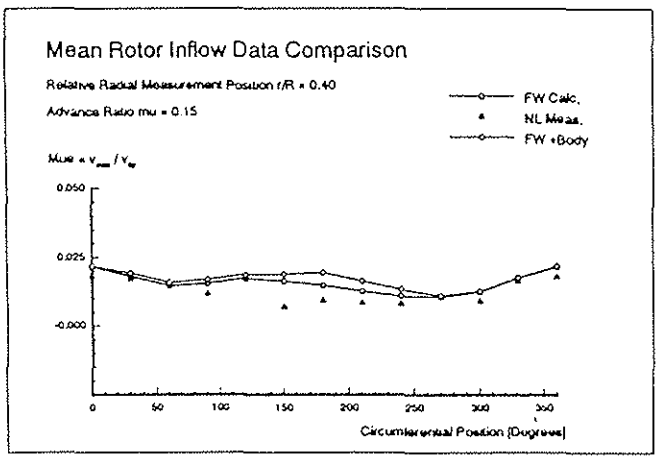

e

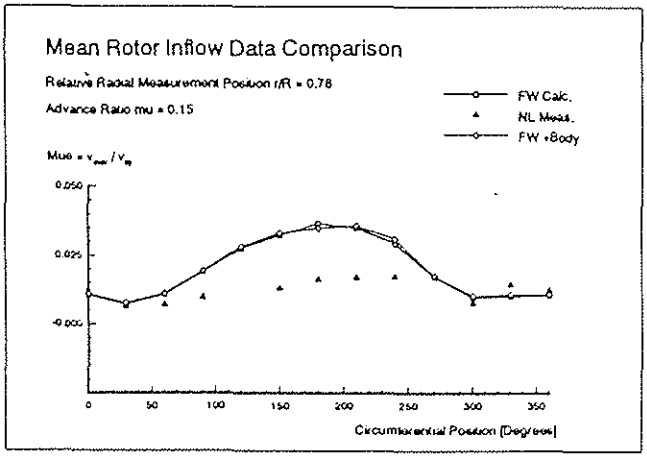

f

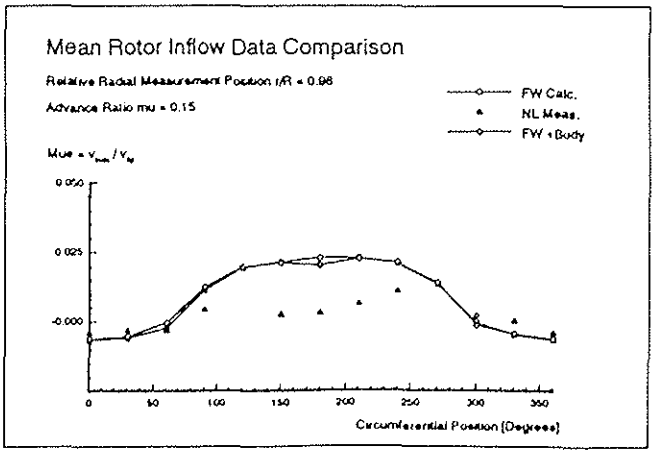

g

Figure 3.13

MUE - Inflow Data

(Parallel to Tip Path Plane and $x_K - z_K$ Plane)
Advance Ratio 0.15